PNAS RESEARCH ARTICLE | ENVIRONMENTAL SCIENCES OPEN ACCESS

Landscape and environmental heterogeneity support coexistence in competitive metacommunities

Prajwal Padmanabha[a,b,1], Giorgio Nicoletti[c,1], Davide Bernardi[a,d,1], Samir Suweis[a,e], Sandro Azaele[a,d,e], Andrea Rinaldo[c,f,2], and Amos Maritan[a,d,e,2]

Affiliations are included on p. 8.

Contributed by Andrea Rinaldo; received June 2, 2024; accepted September 10, 2024; reviewed by David Alonso and Silvia De Monte

Metapopulation models have been instrumental in quantifying the ecological impact of landscape structure on the survival of a focal species. However, extensions to multiple species with arbitrary dispersal networks often rely on phenomenological assumptions that inevitably limit their scope. Here, we propose a multilayer network model of competitive dispersing metacommunities to investigate how spatially structured environments impact species coexistence and ecosystem stability. We introduce the concept of landscape-mediated fitness, quantifying how fit a species is in a given environment in terms of colonization and extinction. We show that, when all environments are equivalent, one species excludes all the others—except the marginal case where species fitnesses are in exact trade-off. However, we prove that stable coexistence becomes possible in sufficiently heterogeneous environments by introducing spatial disorder in the model and solving it exactly in the mean-field limit. Crucially, coexistence is supported by the spontaneous localization of species through the emergence of ecological niches. We show that our results remain qualitatively valid in arbitrary dispersal networks, where topological features can improve species coexistence by buffering competition. Finally, we employ our model to study how correlated heterogeneity promotes spatial ecological patterns in realistic terrestrial and riverine landscapes. Our work provides a framework to understand how landscape structure enables coexistence in metacommunities by acting as the substrate for ecological interactions.

metapopulation dynamics | landscape structure | dispersal networks | optimal channel networks

Significance

The accumulation of field, laboratory, and theoretical evidence has recently clarified the roles of landscape topology and dendritic aggregation as substrates for ecological interactions. They underscore key tasks such as maintaining biodiversity, supporting biological invasions (say, via species-specific dispersal networks) and disease spread (via mobility-driven contact processes). The significant focus placed on a substrate's general viability in supporting a focal species' survival, however, lacks to date a description of how changes in habitat affect the substrate's ability to support coexisting metapopulations of competing species. One thus wonders whether topological features supporting single-species survival may also influence multispecies coexistence and whether disorder and habitat heterogeneity may foster spatial ecological patterns.

Predicting the effect of landscape and habitat changes, including fragmentation, on the dynamics of interacting species is a pressing and paramount challenge (1–3). However, a comprehensive understanding of the key processes that foster biodiversity of ecosystems in the presence of spatial disturbances remains largely elusive to date (4, 5). Though several mechanisms for coexistence and maintenance of biodiversity have been proposed (6–8), studies validating them at a local scale vastly outnumber the spatial counterpart (9, 10). This poses a fundamental limit to our understanding of the composition of ecological communities across spatiotemporal scales and their relation to habitat heterogeneity. Constructing a framework for spatially structured ecosystems is, in general, a formidable and challenging task due to the complexity of species interactions and their role in determining ecosystem stability (11–14), the influence of ever-changing environmental fluctuations shaping population dynamics (15), and the effects of landscape structure (16). Such challenges are complicated by the simultaneous presence of both the short-range dynamics of intra- and interspecific interactions and long-range colonization and migration processes.

In this context, models of metapopulations have proven to be remarkably successful in predicting the survival of a single focal species in complex landscapes of habitat patches interconnected by dispersal networks (17–21). In the presence of colonization and extinction events, the seminal work by Hanski and Ovaskainen (22) has shown that the long-term survival of a species is quantified by a single landscape measure, named metapopulation capacity. The metapopulation capacity is the leading eigenvalue of a suitable landscape matrix, and it subsumes the general viability of a focal species by determining the stability of the persistence-free equilibrium, where the species goes extinct in all patches (23). By developing an individual-based metapopulation model in ref. 24, we have analytically shown that the metapopulation capacity is related to the underlying dispersal pathways through which the species individuals move. Thus, by shaping the landscape and characterizing the relationships between patches, dispersal

Reviewers: D.A., Consejo Superior de Investigaciones Cientificas; and S.D.M., Institute of Biology, École Normale Supérieure Paris.

The authors declare no competing interest.

[1]P.P., G.N., and D.B. contributed equally to this work.

[2]To whom correspondence may be addressed. Email: andrea.rinaldo@epfl.ch or amos.maritan@unipd.it.

This article contains supporting information online at https://www.pnas.org/lookup/suppl/doi:10.1073/pnas.2410932121/-/DCSupplemental.

Published October 22, 2024.

networks act as the template for ecological strategies (25). They drive a population's dynamics, stability, and persistence in both theoretical (11, 26–32) and field studies (33–37). Unaware of these exact results, Tao et al. (38) have independently developed a computational individual-based model that is similarly claimed to be applicable to realistic landscape structures.

Yet, how the interplay among ecological interactions and landscape structures shapes ecological metacommunities is still puzzling (39). The presence of mutualistic and competitive interactions leads to large-scale fluctuations, both at local and mean field scales (40–43), while niche differences arising due to interspecific tradeoffs act as a stabilizing force to promote coexistence (44, 45). Crucially, dispersal may benefit from coexistence (46) and possibly rescue habitats from extinction (47). However, it can also lead to instabilities with unclear effects on diversity (48). Although spatial heterogeneity is generally accepted to favor biodiversity, empirical studies have suggested that it may have both positive and negative effects (49). These contrasting results partly arise due to the complex relationship between the different mechanisms at work in spatially extended ecosystems. At a local scale, mutualistic interactions are necessary to promote coexistence (50–53). However, in a spatial setting, one wonders under what conditions dispersal and spatial structures are beneficial despite competition, or detrimental despite mutualism. This is a fundamental open question to date.

In this work, we address the above shortcomings by developing a general model of ecological metacommunities derived from an underlying individual-level metapopulation description. We focus on the case of species competing for limited space in multiple habitat patches with varying environments. Patches are connected by a dispersal network leading to global colonization dynamics described by an explicit dispersal kernel. We first show that a spatially heterogeneous generalization of Hanski and Ovaskainen's metapopulation capacity fails to predict species' survival in a metacommunity. Rather, by introducing a suitable notion of landscape-mediated fitness, we find that the survival of a species depends on the average fitness of all other species. We analytically prove that, in homogeneous environmental conditions, only the species with the largest fitness survives, and coexistence arises only in a suitable dispersal-extinction trade-off. However, stable coexistence is attainable in sufficiently heterogeneous environments, where habitat patches are distinct from one another, leading to the spontaneous emergence of spatial ecological niches. Although our analytical results are rigorously derived in the mean-field limit of large disordered landscapes, we show numerically that they remain good approximations even for smaller ecosystems with varying spatial structures. In particular, we find that structured dispersal networks are often beneficial to species populations, and that correlated environmental heterogeneity leads to the formation of ecological patterns in realistic terrestrial and aquatic landscapes. Our findings underscore the complex interplay between landscape heterogeneity and species survival and coexistence, offering insights into biodiversity preservation in fragmented habitats.

Results

Multilayer Network Model for Dispersing Metacommunities. We describe the dynamics of S species in a landscape of N interconnected habitat patches, each with a finite number of colonizable sites. We distinguish individuals of each species into sessile individuals settled on a given habitat, and mobile individuals that can explore different patches through a shared or species-specific dispersal network. Model details are given in *Materials and Methods*. In particular, each patch consists of a sink habitat, where the local population would not be able to survive without colonization (54). Within a patch, species do not interact directly but rather compete for the finite number of empty sites available at a given time. This microscopic description corresponds to a multilayer network dynamics of local and global processes occurring at different scales, and it gives rise to the seminal model by Hanski and Ovaskainen (22), as shown in ref. 24. Assuming that the number of colonizable sites is large and that exploration is fast compared to colonization and death (55), we explicitly derive the time evolution of the fraction of space occupied by species α in patch i, $p_{\alpha i}$ as

$$\frac{\mathrm{d}p_{\alpha i}}{\mathrm{d}t} = -e_{\alpha i}p_{\alpha i} + \left(1 - \sum_{\beta=1}^{S} p_{\beta i}\right) \sum_{j=1}^{N} K_{\alpha,ij}\, p_{\alpha j}, \qquad [1]$$

where $e_{\alpha i} > 0$ is the local (within patch) extinction rate of species α in patch i. The species-specific dispersal kernel $K_{\alpha,ij}$ describes colonization by quantifying the rate at which individuals of species α generated from patch j explore the network and eventually colonize patch i. The analytic expression for $K_{\alpha,ij}$ connects it directly to the properties of the underlying dispersal network (*Materials and Methods*). Finally, the term $(1 - \sum_{\beta=1}^{S} p_{\beta i})$ represents the free space in patch i, which introduces competition between species for the finite number of colonizable sites in each habitat.

If only a single focal species were present, the long-time behavior of the system would be determined by a measure called metapopulation capacity. For constant extinction rate e, the seminal work of Hanski and Ovaskainen (22) showed that the metapopulation capacity is the largest eigenvalue λ_M of a suitable landscape matrix determining the global extinction threshold for the focal species. Indeed, if $\lambda_M > e$, the species survives; otherwise, it goes extinct in all patches. In heterogeneous landscapes, where e_i depends explicitly on the patches, we prove instead that survival is possible only when $\lambda > 1$, where λ is the largest eigenvalue of the matrix $\mathbb{K}\mathbb{E}^{-1}$, with $E_{ij} = e_i\delta_{ij}$ (*SI Appendix*). Thus, the metapopulation capacity depends on all e_i at once, which underlines the significance of variations in local extinction rates. This suggests that landscape heterogeneity plays a major role in determining the survival and, as we will show, the coexistence of multiple species. We sketch the model and these ideas in Fig. 1.

Fine-Tuned Coexistence in Homogeneous Landscapes. In Eq. **1**, landscape heterogeneity enters through both the dispersal pathways determining $K_{\alpha,ij}$ and the patch- and species-dependent extinction rates $e_{\alpha i}$. To disentangle their effects, we first consider the homogeneous case in which all habitat patches have the same extinction rate, i.e., $e_{\alpha i} = e_\alpha$ for all i.

Although we can trivially extend the notion of metapopulation capacity for each species λ_M^α, the condition $\lambda_M^\alpha > e_\alpha$ no longer guarantees species survival. Rather, we introduce the concept of average *landscape-mediated* fitness for the α-th species $\langle r_\alpha \rangle = \langle K_\alpha \rangle / e_\alpha$, where $\langle K_\alpha \rangle = N^{-2}\sum_{ij} K_{\alpha,ij}$. $\langle r_\alpha \rangle$ quantifies the balance between colonization and extinction due to the landscape properties, both in terms of the features of habitat patches and the dispersal structure. As we prove in *SI Appendix*, species survival in homogeneous landscapes depends on $\langle r_\alpha \rangle$, and not on the metapopulation capacity. In Fig. 2*A*, we show the phase plot in the (e_1, e_2) space for two species in the homogeneous

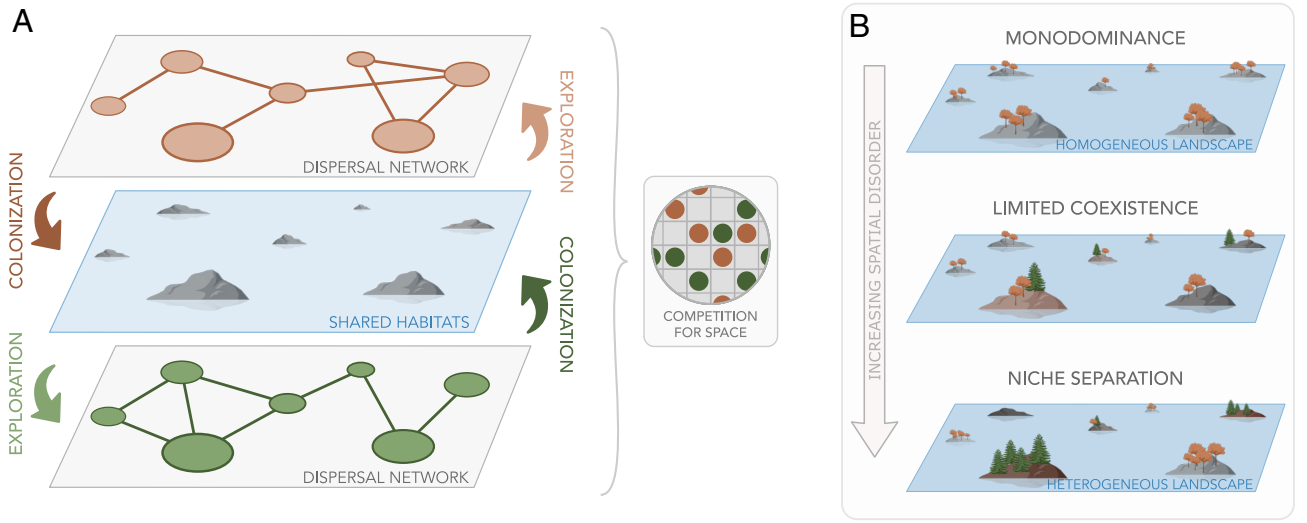

Fig. 1. In a general model of dispersing metacommunities with competition for space, stable coexistence states emerge in heterogeneous landscapes. (*A*) We consider a multilayer dispersal network, where each layer describes the dispersal of a species. Nodes represent shared habitat patches where the species settle and compete for a finite amount of space. (*B*) With dispersal in homogeneous landscapes, where habitat patches are equivalent, only the fittest species survives. However, if landscape heterogeneity is high enough, the coexistence of a large number of species becomes possible through the spontaneous emergence of habitat niches.

case of a grid dispersal network, where the dispersal kernel is invariant under translations. We find that the species with the highest landscape-mediated fitness typically survives in the long-time limit, leading to stable monodominance. However, coexistence is possible by fine-tuning the average landscape-mediated fitnesses to be equal (Fig. 2*A*, solid black line). This requires a precise trade-off between dispersal and extinction, i.e., $\langle K_\alpha \rangle / e_\alpha = \langle K \rangle_\beta / e_\beta$ for all species pairs α, β. As we explicitly prove in *SI Appendix*, this stationary coexistence state is marginally stable, i.e., different stationary states emerge with different initial conditions, a common feature in several models of ecological communities, including metacommunities (56–58). Thus, the patches where a species survives are solely determined by its initial state (Fig. 2*B*).

However, this fine-tuned coexistence is not possible in less homogeneous dispersal networks. In Fig. 2*C* we show the evolution of two species in an Erdős–Rényi dispersal network. Even if their average landscape-mediated fitness is equal, the ecosystem reaches monodominance after displaying a metastable state in which the two species only temporarily coexist. Although the lifetime of this metastable state increases with network size N (*SI Appendix*), it is always one species that survives and colonizes the whole network at stationarity, independently of the initial state. Hence, coexistence in general landscapes is not feasible when all habitat patches are identical.

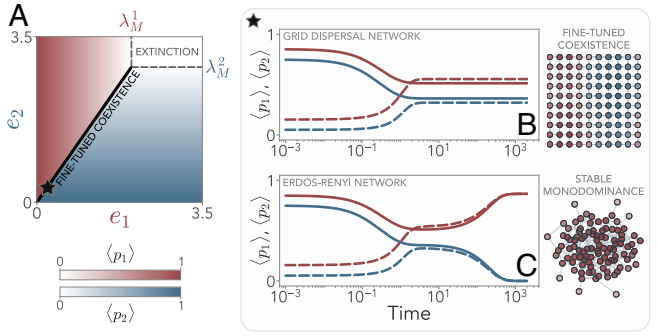

Fig. 2. With homogeneous extinction rates, a single species dominates in the long-time limit, and general stable coexistence is not possible except in a fine-tuned regime. (*A*) Results for a grid dispersal network with two species (red and blue) with extinction rates e_1 and e_2, respectively, equal in all patches. If an extinction rate exceeds the corresponding metapopulation capacity λ_M^α, a species goes extinct (*Upper Right* corner). Coexistence is only possible if the ratio $\langle K_\alpha \rangle / e_\alpha$ is equal for all species (black line), where the average kernel $\langle K_\alpha \rangle$ cannot depend on patches due to the translational invariance of the underlying dispersal network. (B) With an equal ratio for all species, the stationary coexistence state depends on the initial conditions (solid and dashed lines) and corresponds to a central manifold. Note that, since exploration is most effective between neighboring patches, the two species survive in separated regions of the dispersal network. (*C*) In general dispersal networks, the stable state is one in which one species dominates and all others go extinct, independently of the initial conditions. These results hold for a generic number of species (*SI Appendix*). For both these panels the kernels are computed explicitly from the network adjacency matrix (*Materials and Methods*), $e_1 = 0.25$, and e_2 is computed via the central manifold condition.

Stable Coexistence in Heterogeneous Landscapes. To understand how landscape heterogeneity shapes ecosystem diversity, we now turn to the general case in which $e_{\alpha i}$ depends also on the habitat patch i. In order to derive analytical insights, we first consider the mean field limit of the model, where all patches are completely connected in a large ecosystem, i.e., $N \to \infty$. In this scenario, the dispersal kernel reads $K_{\alpha,ij} = K_\alpha / N$ (*Materials and Methods*). The stationary state $p^*_{\alpha i}$ obeys a consistency equation that depends on the local landscape-mediated fitness (LLMF) $r_{\alpha i} = K_\alpha / e_{\alpha i}$, which quantifies the balance between colonization and extinction on each patch rather than across all the patches (*Materials and Methods*). That is, $r_{\alpha i}$ measures how much the interplay between dispersal and local extinction favors the α-th species. If $r_{\alpha i}$ is large, the species is fit for survival on patch i; otherwise, a small $r_{\alpha i}$ denotes that individuals of species α will not be able to effectively colonize patch i. For brevity, we will simply refer to $r_{\alpha i}$ as local fitness. We assume that, for a given species α, the values of $r_{\alpha i}$ are extracted from a generic probability distribution $P_r(r|\vec{\zeta}_\alpha)$, where $\vec{\zeta}_\alpha$ are the species-dependent parameters on which P_r depends.

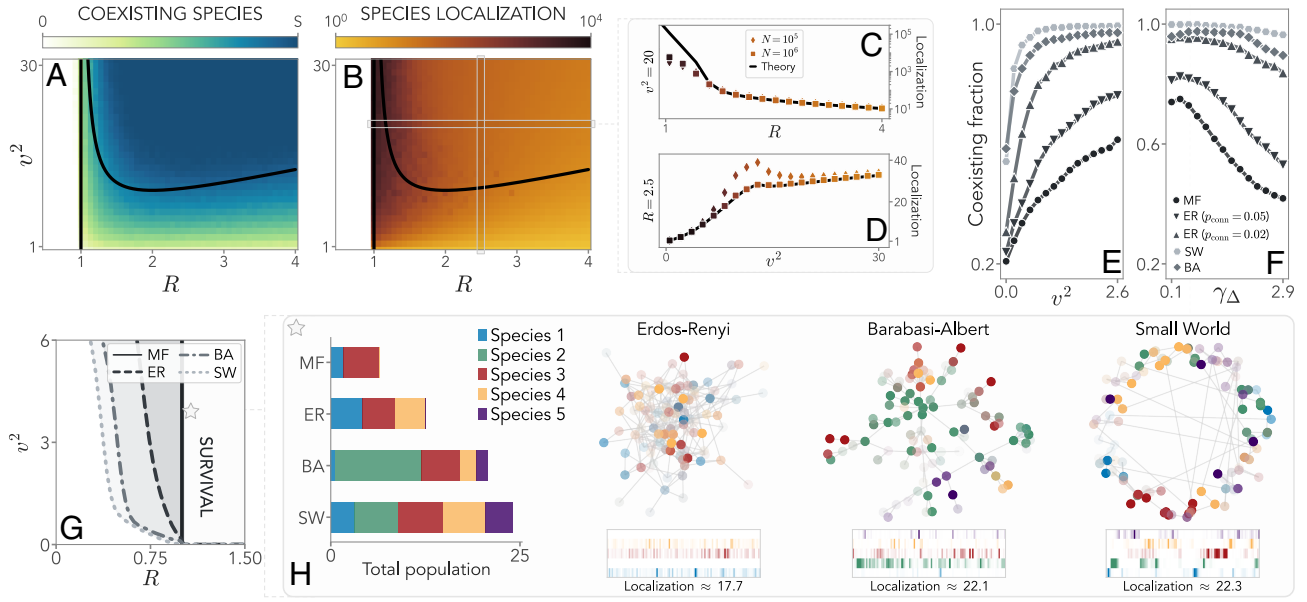

Fig. 3. Strong spatial heterogeneities lead to stable coexistence through the emergence of ecological niches. (*A*) Coexistence in an all-to-all dispersal network with $N = 10^5$ patches and $S = 20$ species, where R is the baseline species fitness and v^2 is the variance of the spatial heterogeneity, which follows a log-normal distribution of mean $\langle r_\alpha \rangle = R + \Delta_\alpha/S$. Coexistence of all species is possible at strong enough heterogeneity, in agreement with theoretical predictions (black lines). Below $R = 1$, no species can survive. Here, we take Δ_α to be evenly spaced between $\pm 5/2$, so that $\gamma_\Delta = 2.5$. (*B*) Coexistence is enabled through species localization (computed via the inverse participation ratio, *Materials and Methods*), signaling the spontaneous emergence of ecological niches. (*C*) Close to the extinction line at $R = 1$, species become strongly localized in a few habitat patches, as predicted by the theory in the $N \to \infty$ limit. (*D*) For large ecosystems, localization increases with the heterogeneity variance v^2. At low enough N, localization displays a local peak at intermediate values of the variance due to finite-size effects. (*E*) The fraction of coexisting species, at constant average fitness, strongly depends on the topology of the dispersal network. Small-world (SW) and Barabasi–Albert (BA) networks allow for the coexistence of more species at lower values of the variance. Here, $R = 2$, $\gamma_\Delta = 1$, $S = 5$, and $N = 100$. (*F*) As the species become more different and γ_Δ increases, it becomes harder to sustain them and topology plays a fundamental role in determining their coexisting fraction. Parameters are as in the previous panel, with $v^2 = 3$. We note that, due to finite-size effects, in the mean-field case, we do not find that all species coexist when γ_Δ is small. (*G*) At $\gamma_\Delta = 0$, the average fitness across species is equal. We find through numerical simulations that the topology of dispersal networks affects the extinction transition ($R = 1$ in the mean-field case), allowing for a broader region of survival. (*H*) Diversity and localization increase in complex dispersal networks, with Barabasi–Albert and small-world networks displaying a higher total population. Color transparency corresponds to the population density in the patch, and the bar plot below each network shows the population density in each species for each patch. Simulations and parameters of the dynamical model are specified in *Materials and Methods*.

P_r describes the landscape heterogeneity in terms of habitat-dependent colonization and extinction.

For a large ecosystem, Eq. **9** can be solved exactly as a $1/S$ expansion for the stationary state. For simplicity, we consider the case in which all species have the same landscape-mediated fitness variance, $\sigma_r^2 = v^2$, which quantifies the strength of the landscape heterogeneity. We also take the mean of P_r to scale as $\langle r_\alpha \rangle = R + \Delta_\alpha/S$, where R sets the baseline LLMF, and the vector $(\Delta_1, \ldots, \Delta_S)$ measures the deviation of each species from such baseline. As we show in *Materials and Methods*, when S is sufficiently large, the coexistence of all species becomes possible only if:

$$R > 1 \quad \text{and} \quad v^2 > v_c^2 := \gamma_\Delta \frac{R^2}{R-1}. \qquad [2]$$

independently on the choice of the fitness distribution. The parameter $\gamma_\Delta = \sum_{\alpha=1}^{S} \Delta_\alpha/S - \min_\alpha \Delta_\alpha$ determines the extent to which species are different from one another. The first of the two conditions in Eq. **2** indicates that the baseline must be large enough to allow for coexistence. The second, instead, sets a minimal level of heterogeneity, which must exceed a critical value v_c^2. The more species are diverse, the larger γ_Δ and the more heterogeneous the landscape needs to be for them to survive. Notably, when the average LLMF is identical for all species $\gamma_\Delta = 0$, this implies that $v_c^2 = 0$ and coexistence is guaranteed whenever $R > 1$. In Fig. 3*A*, we show the number of coexisting species in the (R, v^2) phase space for a given choice of Δ_α and a log-normal distribution for P_r, obtained numerically for a finite number of habitat patches and species. The results are in excellent agreement with the theoretical prediction (black lines). Numerical simulations suggest that this coexistence solution is unique, and corresponds to stationary values of the populations that do not depend on the initial conditions, contrary to the case of homogeneous landscapes.

In particular, no species survives if $R < 1$, as the baseline is too small to support survival. For $R > 1$, full coexistence becomes possible at large enough landscape heterogeneity. Remarkably, the critical variance diverges also for $R \to \infty$. In this scenario, all species have very high baseline LLMF and thus they can grow easily in all habitat patches, regardless of the variance. As a consequence, competition is widespread, effectively hindering coexistence, which is instead optimal at intermediate values of R. These results suggest that the coexistence state does not correspond to species densities that are evenly spread throughout the landscape. We measure this effect by computing how localized each species is (*Materials and Methods*), which we plot in Fig. 3 *B*–*D*. At fixed v^2, we find indeed that localization decreases with R, as larger baselines allow species to grow in more habitat patches—thus increasing competition and making coexistence harder. On the other hand, as the ecosystem approaches the $R = 1$ line, localization drastically increases. This phenomenon is well predicted by the theory and has profound ecological and physical consequences, as the boundary at $R = 1$ marks a sharp transition toward widespread extinction. To be able to survive near this threshold, species must maximize their segregation, as any amount of competition would push them to extinction.

At fixed R, instead, localization increases with the variance of LLMF. Once more, this is due to the fact that, at higher v^2, the heterogeneity of the landscape forces the species to become more and more segregated. In doing so, competition is reduced, as the largest share of each species is concentrated within a fraction of the available habitat patches, benefiting coexistence. From an ecological perspective, this result shows that a stronger landscape heterogeneity fosters the spontaneous emergence of ecological niches. Such emergence can be understood in terms of a trade-off between species needing the baseline R large enough to survive, but small enough to allow landscape heterogeneity to minimize competition. As a consequence, by localizing their population in those patches where they are fitter, species survive in niches that buffer the detrimental effect of competition for space, as measured by the local landscape-mediated fitness.

Landscape Structure Promotes Coexistence. Our analytical results have been obtained for an all-to-all dispersal network, and in the limit of a large spatial ecosystem, i.e., $N \to \infty$. We now study the effect of small N and S and the impact of network motifs by comparing the mean-field (MF) scenario with three prototypical networks: Erdős–Rényi (ER) networks at two different connectances, introducing network sparsity; Barabàsi-Albert (BA) networks, characterized by hubs; and small-world (SW) networks, with high clustering coefficient (59). To compare the effects of different dispersal topologies, we keep the mean LLMF $\langle r_\alpha \rangle$ for each species constant, which results in similar single-species survivability across different networks (*Materials and Methods*).

We find that our results remain qualitatively valid, with the fraction of coexisting species increasing with landscape heterogeneity across all networks (Fig. 3*E*). However, the dispersal structure quantitatively shifts the coexistence transition. ER networks display enhanced coexistence with increasing sparsity (Fig. 3*E*), a trend further detailed in *SI Appendix*. At a fixed sparsity, coexistence is also boosted by the introduction of hubs or small-world topological features. In Fig. 3*F*, we also show that complex dispersal networks can also sustain more diverse coexisting species, with higher γ_Δ for the same variance of the landscape-mediated fitness.

We further consider the case of neutral species with equal LLMF on average, given by $\gamma_\Delta = 0$. In this way, we remove the disadvantage due to intrinsic fitness differences, as all species share the same baseline R, and coexistence is solely driven by the distribution's variance (*Materials and Methods*). Thus, we focus on how the extinction transition changes from the mean-field case at $R = 1$. In Fig. 3*G*, we show that changing the topology shifts the extinction transition line, allowing for survival with less spatial heterogeneity. Indeed, for the same realization of $r_{\alpha i}$, structured landscapes such as SW and BA networks support a larger number of species as well as a higher total population (Fig. 3*H*). Interestingly, although all species in this example have the same average fitness, the interplay between spatial heterogeneity and the given dispersal network structure determines which species survive, leading to uneven population distributions. For instance, the second species in Fig. 3*H* becomes dominant in the BA network because of its higher LLMF within the largest hub. Hence, landscape structure plays a fundamental role in shaping species' survival when dispersal and colonization are both taken into account. Depending on the interplay between LLMF and dispersal topology, a species may thrive in a given network but go extinct in another. Importantly, the presence of the coexistence transition across different networks shows that our exact results are still qualitatively valid well beyond the mean-field case.

Spatial Patterns in Heterogeneous Landscapes with Correlated Habitats. Realistic landscapes not only consist of structured dispersal networks, but of spatial correlation in environmental factors as well. To investigate our results under this constraint, we introduce a correlation between a species' LLMF in the habitat patch i and patch j which decreases with distance, with a typical correlation length of d_{corr} (*Materials and Methods*). We also consider two realistic landscapes with intrinsic spatial structures: terrestrial and aquatic. We model terrestrial landscapes using random geometric graphs (RGGs) (60). Each habitat patch is embedded in a random spatial position, and the patches are connected if their Euclidean distance is smaller than a given threshold. Furthermore, exploration through these dispersal pathways is inversely proportional to their distance. In Fig. 4*A*, we show that, on average, a larger correlation length between habitat patches increases the total population in the ecosystem. This increase is fostered by a spatial clustering of niches, such that the same species occupies habitat patches that are close together (Fig. 4 *B* and *C*), making colonization more efficient overall and thereby also reducing interspecies competition.

The features of aquatic landscapes, instead, have been extensively shown to be well-captured by theoretical constructs termed optimal channel networks (OCNs) (4, 61, 62). In this case, patches represent fluvial habitats connected by a river network flowing from high to low elevations, and recapitulated by aggregated pathways, i.e., the total contributing area at-a-

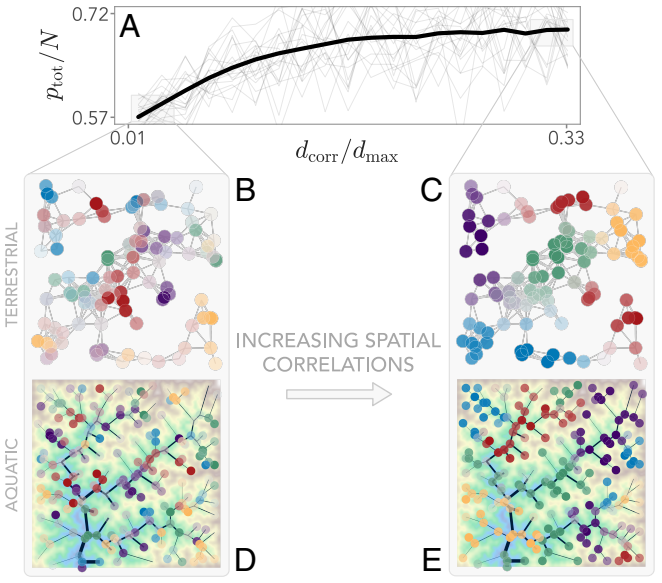

Fig. 4. Effect of spatially correlated heterogeneity in niche formation. (*A*) The total population p_{tot} increases with the spatial correlation length over the maximum distance between nodes, $d_{\text{corr}}/d_{\text{max}}$. (*B* and *C*) We first study the effect of spatial correlations on terrestrial landscapes, modeled through a random geometric graph (RGG). The correlation decays with the Euclidean distance between the nodes and allows for the spatial clustering of niches. As a result, nodes that are close together in space are occupied by the same species (different node colors represent different species). (*D* and *E*) In aquatic landscapes, obtained via optimal channel networks (OCNs), spatial correlations decay instead with the network distance. Now, niches for different species spontaneously emerge in different river branches, since nodes that are spatially close to each other may be at large network distances. The shaded terrain map represents the elevation map obtained from the OCN. The definition and parameters of the networks are reported in *Materials and Methods*.

site (63), the master variable of fluvial geomorphology (64) (*Materials and Methods*). We assume that the correlation between species LLMF decays with the network distance rather than the Euclidean one, which quantifies the dendritic connections along the river network. In Fig. 4 *D* and *E*, we see that again correlations induce the emergence of spatial ordering. This time, nearby spatial regions may be occupied by different species, as spatially close habitat patches may be distant along the river network. Thus, the emergent ecological patterns in space intrinsically reflect the underlying landscape structure.

Discussion

In this work, we studied a general theoretical framework to characterize coexistence in ecosystems dominated by dispersal, induced by the connectivity of habitat patches. We find that stable coexistence is favored in heterogeneous landscapes, where it is enabled by the spontaneous emergence of ecological niches that minimize direct competition. The topological and spatial structure of dispersal networks may help coexistence, therefore playing a pivotal role in shaping the features of dendritic ecosystems. Crucially, our results suggest that a sufficient degree of landscape heterogeneity is essential for sustaining biodiversity.

In homogeneous networks and environments, we find that dispersal can foster a large degree of diversity of coexisting species when it is fine-tuned to be in a trade-off with local extinction. However, even small perturbations from this fine-tuned coexistence lead to dispersal promoting interspecific competition, thereby ultimately leading to monodominance. As in our model monodominance arises due to competition for space, this is reminiscent of the competitive-exclusion principle, implying that the number of species cannot exceed the number of resources (65). Yet, in the presence of spatial heterogeneity, we have shown that coexistence in different habitat patches is possible in landscapes with strong heterogeneity, as measured by a suitably defined landscape-mediated fitness. Indeed, in this case, habitat patches may be viewed as multiple resources arising from landscape heterogeneity, allowing for large-scale coexistence without violating the competitive exclusion principle.

Further, our results demonstrate that dispersal can act as a stabilizing force in general metacommunities. This applies when the underlying substrate for dispersal and ecological interactions acts synergistically with landscape heterogeneity to reduce interspecific competition (66–68). In particular, the structure of dispersal networks may enable broader niche creation and reduce competition, and realistic terrestrial or aquatic networks lead to the emergence of characteristic spatial patterns in correlated environments. Indeed, weak and sparse interactions in local communities have been shown to be beneficial to coexistence (66), with the topology of interactions playing a driving role in the stability of metacommunities (69). Although our considerations are limited to spatial competition, they provide a baseline for the impact of dispersal, allowing future works to incorporate it alongside direct ecological interactions among species (44). Importantly, one of the key predictions of our model is that, as the landscape parameters are driven toward widespread extinction, species localization will rapidly increase. This is akin to typical early warning signals of critical transitions in ecological systems (70), possibly serving as an indicator of the health of the ecosystem.

In the last twenty years, it has become clear that dispersal mechanisms can fundamentally alter the structure of ecosystems, both with and without disorder. In this context, our framework allows for deeper insight into quantitative characterizations of individual-level processes underlying colonization and extinction, while being simple enough to allow for analytical treatment. As such, several extensions could be readily considered, allowing for in-depth characterizations of specific ecosystems. Expanding the multilayered network model to include other interactions, such as mutualism and predation would help us better understand the role of dispersal in mediating intra- and interspecific competition. Moreover, the addition of migration of new species is an interesting extension that would allow for diversification and community turnover, where the absence of the extinction transition may lead to richer temporal dynamics (43). Apart from demonstrating a natural extension of metapopulation models to metacommunities, our framework can be generalized to account for different biological behavior both in plants and animals, for instance, organisms with life-history stages such as sessile adults and mobile juveniles or motile and nonmotile subgroups within a given life-history stage. The presented microscopic model is immediately malleable to include such additional effects. Overall, our approach will enable us to study how landscape structure affects cooperation and competition between different ecological niches, a pressing matter in understanding how biodiversity evolves under environmental changes.

Materials and Methods

Metacommunity Model with Dispersal. We start from an individual-based dynamics describing S species in N interconnected habitat patches. Each species, in principle, may explore the patches differently, according to its dispersal pathways, so that the overall dispersal network is a multilayer network, with each layer corresponding to a given species. For simplicity, here we assume that all species share the same dispersal network, but our framework can be immediately generalized to other cases. Each habitat patch has a finite number M of colonizable sites. We denote with $P_{\alpha i}$ a sessile individual of the α-th species, that settled in a site of patch i. As in typical metapopulation models (22), the local habitat follows a sink dynamics, where sessile individuals can only go extinct with a rate $e_{\alpha i}$. However, species can explore the dispersal network by giving rise to mobile offspring, denoted with $X_{\alpha i}$, which move between habitat patches before settling. When settling, if an empty space is encountered, settlement is successful. However, if an occupied site is encountered, settlement fails and the explorer dies. The model is described by the microscopic reactions

$$\begin{aligned}
&\text{Death of settled individual}: \quad P_{\alpha i} \xrightarrow{e_{\alpha i}} \varnothing_i,\\
&\text{Creation of explorers}: \quad P_{\alpha i} \xrightarrow{h_\alpha A_{ij}} P_{\alpha i} + X_{\alpha j},\\
&\text{Diffusion of explorers}: \quad X_{\alpha i} \xrightarrow{D_\alpha A_{ij}} X_{\alpha j},\\
&\text{Successful colonization}: \quad X_{\alpha i} + \varnothing_i \xrightarrow{\lambda_\alpha/M} P_{\alpha i},\\
&\text{Unsuccessful colonization}: \quad X_{\alpha i} + P_{\beta i} \xrightarrow{\lambda_\alpha/M} P_{\beta i},
\end{aligned} \qquad [3]$$

where D_α and λ_α are respectively the exploration and settling rate for species α, h_α is the feasibility of exploration of the species, and A_{ij} is the adjacency matrix of the dispersal network that connects habitat patches. In particular, we assume that mobile individuals are created in neighboring patches to avoid self-colonization of the same patch. These explorers move along the landscape through the dispersal network until they attempt to colonize one of the sites in their current habitat patch, either successfully settling on an empty site or dying in the process.

This model is the natural multispecies generalization of seminal metapopulation models, as it reduces to that of Hanski and Ovaskainen in the case of a single focal species (22). Indeed, as in previous works (24), we can obtain an explicit metapopulation model in the limit of fast exploration (55). If $p_{\alpha i} = \langle P_{\alpha i} \rangle / M$, we

can derive Eq. **1** exactly from the leading order of the Kramers–Moyal expansion of the master equation (*SI Appendix*) (71). In particular, the kernel is given by the matrix

$$K_{\alpha\beta,ij} = \delta_{\alpha\beta} h_\alpha \sum_{l=1}^{N} A_{jl} \sum_{k=1}^{N} \frac{V_{ik}(V^{-1})_{kl}}{1 + f_\alpha \omega_k}, \quad [4]$$

where ω_k is the k-th eigenvalue of the transpose outdegree Laplacian of the dispersal network, and V_{ij} is the matrix of its right eigenvectors. The parameter $f_\alpha = D_\alpha/\lambda_\alpha$ represents the exploration efficiency of species α - if $f_\alpha \gg 1$, explorers will visit many habitat patches before attempting colonization, whereas if $f_\alpha \ll 1$ they will remain close to the originating patch. In simulations of the model, we typically set $h_\alpha = \xi_\alpha/(1 + f_\alpha^{-1})$, with ξ_α the maximal dispersal capacity of the species (24). In this way, we ensure that exploration is not possible as $f_\alpha \to 0$, and that $f_\alpha \to \infty$ gives a finite kernel.

We would like to stress that the presented microscopic model is a generalization of the single-species metapopulation model corresponding to that of Hanski and Ovaskainen (22). However, modifying the underlying reactions to include other life-history stages or different explorer creation-colonization dynamics can still lead to qualitatively similar macroscopic models in terms of the density of the settled individuals, albeit with different characteristics of the dispersal kernel.

Mean-Field Dispersal Kernel. In a mean-field network, we write the adjacency matrix as $A_{ij} = (1 - \delta_{ij})/N$, which, in the fast exploration limit, is equivalent to rescaling the maximal dispersal capacity as $\xi_\alpha \to \xi_\alpha/N$. Then, the kernel elements are given by

$$K^{\mathrm{MF}}_{\alpha,ij} = h_\alpha \left[\frac{(N-1)f_\alpha}{1 + N f_\alpha} \delta_{ij} + \frac{1 + (N-1)f_\alpha}{1 + N f_\alpha} \left(1 - \delta_{ij}\right) \right]$$

so that, in the large N limit, we find that $K_{\alpha,ij} = K_\alpha/N$ for all edges i and j, with $K_\alpha = \xi_\alpha/(1 + f_\alpha^{-1})$.

Fine-Tuned Coexistence. We consider a homogeneous landscape, where all habitat patches have the same extinction rate e_α for a given species, and the dispersal network is invariant under translations. In this scenario, the stationary species density cannot explicitly depend on the habitat patches, so $p^*_{\alpha i} = p^*_\alpha$. A solution $p^*_\alpha > 0$ must obey the self-consistency equation

$$1 - \sum_{\beta=1}^{S} p^*_\beta = \frac{e_\alpha}{N \langle K_\alpha \rangle}, \ \forall \alpha = 1, \ldots, S, \quad [5]$$

where $\langle K_\alpha \rangle = N^{-2} \sum_j K_{\alpha,ij}$ does not depend on i due to the underlying translational invariance. Thus, coexistence is possible if and only if the average species LLMF $\langle r_\alpha \rangle = \langle K_\alpha \rangle / e_\alpha$ is identical for all species. In *SI Appendix*, we prove that this stationary solution corresponds to a zero eigenvalue of the Jacobian, and thus is a central manifold. Hence, this comprises a family of stationary solutions that explicitly depend on the initial condition, which disappears in the absence of translational invariance.

General Solution in Heterogeneous Landscapes. The mean-field equation corresponding to Eq. **1** are given by

$$\dot{p}_{\alpha i} = e_{\alpha i} \left[-p_{\alpha i} + \left(1 - \sum_{\beta=1}^{S} p_{\beta i}\right) r_{\alpha i} \langle p_\alpha \rangle \right], \quad [6]$$

where $\langle p_\alpha \rangle = \sum_{j=1}^{N} p_{\alpha j}/N$, and we introduced the local species fitness $r_{\alpha i} = K_\alpha / e_{\alpha i}$. The stationary values $p^*_{\alpha i}$ must obey the consistency equation

$$1 = \frac{1}{N} \sum_{i=1}^{N} r_{\alpha i} \left(1 + \sum_{\beta=1}^{S} r_{\beta i} \langle p^*_\beta \rangle\right)^{-1}. \quad [7]$$

We assume that $r_{\alpha i}$ are quenched random variables extracted from a distribution $P_r(r|\vec{\zeta}_\alpha)$, where $\vec{\zeta}_\alpha$ are species-dependent parameters. In *SI Appendix*, we show that the consistency equation can be rewritten in terms of the moment-generating function of the distribution of local fitness

$$W_\alpha(\omega) = \int_0^\infty \mathrm{d}r \, P_r(r|\vec{\zeta}_\alpha) \, e^{-r\omega} \quad [8]$$

as

$$1 = S \int_0^\infty \mathrm{d}z e^{-S\bar{F}(z,\vec{x})} \left(-\frac{W'_\alpha(z\,x_\alpha)}{W_\alpha(z\,x_\alpha)} \right), \quad [9]$$

where $x_\alpha = S \langle p^*_\alpha \rangle$, $W_\alpha(\omega)$ is the moment generating function of $P_r(r|\vec{\zeta}_\alpha)$ and $\bar{F}(z,\vec{x}) = z - \frac{1}{S} \sum_{\beta=1}^{S} \ln W_\beta(z\,x_\beta)$. In particular, we take the average to scale as $\langle r_\alpha \rangle = R + \Delta_\alpha/S + \mathcal{O}(1/S^2)$, where R is the baseline LLMF and Δ_α represent the deviation from such baseline. Then, the rescaled average stationary population $x_\alpha = S \langle p^*_\alpha \rangle$ obeys

$$x_\alpha = \frac{\Delta_\alpha - H}{v_\alpha^2} R + \mathcal{O}\left(\frac{1}{S}\right), \quad [10]$$

where $v_\alpha^2 = \left\langle r_\alpha^2 \right\rangle - \langle r_\alpha \rangle^2$, and

$$H = \left(\overline{\frac{1}{v^2}} \right)^{-1} \left[\left(\overline{\frac{\Delta}{v^2}} \right) - \frac{R-1}{R^2} \right] \quad [11]$$

with $\bar{y} = S^{-1} \sum_\beta y_\beta$ denotes the average over disorder (*SI Appendix*). Thus, from Eq. **10**, we have that coexistence is possible if $\Delta_\alpha > H$, which reduces to the set of conditions in Eq. **2** if we take $v_\alpha^2 = v^2$ for all species α. In general, we immediately see that at large disorder variance, it is easier to satisfy the coexistence condition. All plots in the mean-field case are obtained by explicitly solving the consistency equation.

Species Localization and Ecological Niches. We compute species localization through the inverse participation ratio (IPR), defined as

$$NI_\alpha = \frac{\left\langle p_\alpha^4 \right\rangle}{\left\langle p_\alpha^2 \right\rangle^2}. \quad [12]$$

If a species is present prevalently in $k < N$ habitat patches, then it is easy to show that the IPR is $NI_\alpha \approx N/k$. Hence, if a species is not localized, we expect $NI_\alpha \approx 1$, whereas if it is present in only one habitat patch we have $NI_\alpha \approx N$. Therefore, the IPR is a measure of localization and thus of how much species survival relies on the emergence of ecological niches. In Fig. 3*B*, we plot the average $S^{-1} N \sum_\alpha I_\alpha$. In *SI Appendix*, we show that the IPR can be computed exactly as

$$NI_\alpha = \frac{1}{6} \frac{\int_0^\infty dz\, z^3 \, e^{-S\bar{F}(z,x)} W^{(4)}(zx_\alpha)/W(zx_\alpha)}{\left[\int_0^\infty dz\, z\, e^{-S\bar{F}(z,x)} W^{(2)}(zx_\alpha)/W(zx_\alpha)\right]^2}, \quad [13]$$

where $W^{(m)}$ is the m-th derivative of the moment-generating function, and $\bar{F}$ has been defined in the main text.

Dynamics in Arbitrary Dispersal Networks. In an all-to-all dispersal network, the kernel does not depend on the habitat patches and the system solely depends on the average species LLMF. However, this is not true in general, as the dispersal kernel in Eq. **4** has been shown to depend on all possible paths between pairs of patches (24). In this scenario, the local species fitness is $r_{\alpha i} = N \langle K_\alpha \rangle / e_{\alpha i}$, where the N prefactor comes from the rescaling $\xi_\alpha \to \xi_\alpha/N$. This definition immediately reduces to the mean-field case when we consider an all-to-all network, and once more can be interpreted as a local balance between colonization and extinction.

To integrate numerically the dynamics in an arbitrary dispersal network, which depends explicitly on the extinction rates, we consider first a quenched realization of the disordered local species fitnesses $r_{\alpha i}$. Then, for each species α, we compute the kernel elements $K_{\alpha,ij}$ and its average $\langle K_\alpha \rangle = N^{-2} \sum_{ij} K_{\alpha,ij}$, from which we can get the extinction rates as $e_{\alpha i} = N \langle K_\alpha \rangle / r_{\alpha i}$. Notice that this explicitly shows that, in order to maintain the average $\langle r_\alpha \rangle$ constant, the extinction rates must be tuned in response to the specific kernel, i.e., to the topology of the dispersal network. In particular, in Fig. 3*H*, we take the parameters of the log-normal distribution for the local species fitness to be $\langle r \rangle = R = 1$, $v^2 = 1.5$. The kernel for each species is computed as in Eq. **4**, with $\xi_\alpha = 1/N$ and f_α to be uniformly spaced in [0.5, 2]. To highlight the effect of the network structure, the disorder realization is kept fixed across the different topologies.

Terrestrial and Aquatic Landscapes. To model realistic terrestrial landscapes, we consider RGGs (60). RGGs are generated by sampling N patches uniformly in the unit square, i.e., each patch has a spatial position $(x_i, y_i) \in [0, 1] \times [0, 1]$. Two patches are connected if their Euclidean distance d_{ij} is smaller than a given threshold d_{th}. We set $d_{\text{th}} = 0.17$ for Fig. 4, but our results are qualitatively independent of this choice, provided that the network is connected and not dense. In this spatially embedded network, we take the weights of each edge to be functions of the distance between the patches, i.e., we write the adjacency matrix as

$$A_{ij} = \frac{d_{\min}}{d_{ij}} \in [0, 1], \qquad [14]$$

where $d_{\min}$ is the minimum distance between two patches of the network. In this way, the exploration rate in Eq. **3** decreases for habitats that are far apart.

Aquatic and riverine landscapes, instead, are well modeled by OCNs (4, 61, 62). An OCN is a spanning tree where each node is associated with a slope-area law relating the elevation h_i and the local drainage area $\mathcal{A}_i$ (63, 64, 72), related to one another by the scaling relation $|\nabla h_i| \propto \mathcal{A}_i^{\gamma-1}$, with the scaling exponent $\gamma = 1/2$. For a given adjacency matrix A_{ij}, the areas are given by $\mathcal{A}_i = \sum_j W_{ji} \mathcal{A}_j + 1$ (a unit pixel size is conventionally assumed, i.e., the random variable $\mathcal{A}$ is concentrated in the domain $(1, \mathcal{A}_{\max})$, characterized by a universal probability distribution $p(\geq a) = a^{-\beta} \mathcal{F}(a/\mathcal{A}_{\max})$, where: $\beta = 0.43 \pm 0.2$, and $\mathcal{F}(x) = 0$ for $x \to \infty$ and $\mathcal{F}(\to 0)$ is a constant (62, 64). An OCN then is a spanning tree that reaches a dynamically accessible local minimum of the total energy dissipation functional $E_{\text{OCN}} = \sum_i \mathcal{A}_i^\gamma$ (64). This proves to be an exact property of the general landscape evolution equation under reparameterization invariance and in the limit of the small gradient approximation (73). In particular, in Fig. 4, the OCN has been aggregated so that each pixel represents either a source, an outlet, or a confluence (74). In the case of OCNs, the relevant distance that we use to build the metacommunity model is not the Euclidean distance as for RGGs, but rather the alongstream network distance (also known as chemical distance).

Spatially Correlated Disorder. To study the case of spatially correlated disorder, we start from distance matrix d_{ij}–either Euclidean distance for RGGs or network distance for OCNs. Then, we parameterize the covariance Σ_{ij} between two habitat patches i and j as

$$\Sigma_{ij} = \left[1 - \left(\frac{m_1 d_{ij}}{m_2}\right)^2\right] \exp\left[-\frac{\left(m_1 d_{ij}\right)^2}{2m_3^2}\right] \qquad [15]$$

which is a Ricker wavelet and allows for both local correlations and long-range anticorrelations. Then, the local species fitness is distributed as a multivariate log-normal distribution, i.e., $r_{\alpha i} = e^{y_{\alpha i}}$ with $y_{\alpha i}$ a multivariate Gaussian variable $y_{\alpha i} \sim \mathcal{N}(\vec{\mu}, \hat{\Sigma})$. For Fig. 4, we take $\mu_i = 0.5$ and set $m_1 = 3$, $m_2 = 1.3$, and $m_3 = 1$ for RGGs–resulting in small anticorrelations at long distances–and $m_1 = 0.8$, $m_2 = 5$, and $m_3 = 1$ for OCNs–resulting in positive and exponentially decaying correlations with the network distance. The emergence of spatial patterns is qualitatively independent of these choices, with the only constraint being that $\hat{\Sigma}$ must be a semipositive-definite matrix. In Fig. 4, we take the mean of the multidimensional log-normal distribution to be $\mu_i = 0.5$ for all patches. The simulation of the dynamics for each network is performed with the parameters described above.

Data, Materials, and Software Availability. There are no data underlying this work.

ACKNOWLEDGMENTS. G.N. and A.R. acknowledge funding provided by the Swiss NSF through its Grant CRSII5_186422. D.B., A.M., and S.A. acknowledge the support of the Italian Ministry of University and Research (project funded by the European Union–Next Generation EU: "PNRR Missione 4 Componente 2, 'Dalla ricerca all'impresa,' Investimento 1.4, Progetto CN00000033"). S.S. acknowledges financial support under the National Recovery and Resilience Plan, Mission 4, Component 2, Investment 1.1, Call for tender No. 104 published on February 2, 2022 by the Italian Ministry of University and Research (MUR), funded by the European Union–Next Generation EU–Project Title: Anchialos: diversity, function, and resilience of Italian coastal aquifers upon global climatic changes–CUP C53D23003420001 Grant Assignment Decree no. 1015 adopted on July 7, 2023 by the Italian MUR.

Author affiliations: [a]Department of Physics and Astronomy "Galileo Galilei," University of Padova, Padova 35131, Italy; [b]Department of Fundamental Microbiology, University of Lausanne, Lausanne 1015, Switzerland; [c]Laboratory of Ecohydrology, School of Architecture, Civil and Environmental Engineering, École Polytechnique Fédérale de Lausanne, Lausanne 1015, Switzerland; [d]National Biodiversity Future Center, Palermo 90133, Italy; [e]Istituto Nazionale di Fisica Nucleare, Sezione di Padova, Padova 35131, Italy; and [f]Department of Civil, Environmental and Architectural Engineering, University of Padova, Padova 35131, Italy

Author contributions: P.P., G.N., D.B., S.S., S.A., A.R., and A.M. designed research; P.P., G.N., D.B., S.S., A.R., and A.M. performed research; P.P., G.N., D.B., and S.A. analyzed data; and P.P., G.N., D.B., S.S., S.A., A.R., and A.M. wrote the paper.

1. G. Ceballos *et al*., Accelerated modern human-induced species losses: Entering the sixth mass extinction. *Sci. Adv.* **1**, e1400253 (2015).
2. D. Tilman *et al*., Future threats to biodiversity and pathways to their prevention. *Nature* **546**, 73–81 (2017).
3. F. Isbell *et al*., Linking the influence and dependence of people on biodiversity across scales. *Nature* **546**, 65–72 (2017).
4. A. Rinaldo, M. Gatto, I. Rodriguez-Iturbe, *River Networks As Ecological Corridors. Species, Populations, Pathogens* (Cambridge University Press, New York, 2020).
5. R. Durrett, S. Levin, Stochastic spatial models: A user's guide to ecological applications. *Philos. Trans. R. Soc. Lond. Ser. B Biol. Sci.* **343**, 329–350 (1994).
6. P. Chesson, Mechanisms of maintenance of species diversity. *Annu. Rev. Ecol. Syst.* **31**, 343–366 (2000).
7. M. Loreau, C. De Mazancourt, Biodiversity and ecosystem stability: A synthesis of underlying mechanisms. *Ecol. Lett.* **16**, 106–115 (2013).
8. S. A. Levin, Multiple scales and the maintenance of biodiversity. *Ecosystems* **3**, 498–506 (2000).
9. A. D. Bjorkman *et al*., Plant functional trait change across a warming tundra biome. *Nature* **562**, 57–62 (2018).
10. J. HilleRisLambers, P. B. Adler, W. S. Harpole, J. M. Levine, M. M. Mayfield, Rethinking community assembly through the lens of coexistence theory. *Annu. Rev. Ecol. Evol. Syst.* **43**, 227–248 (2012).
11. R. S. Etienne, D. Alonso, A dispersal-limited sampling theory for species and alleles. *Ecol. Lett.* **8**, 1147–1156 (2005).
12. S. Allesina, S. Tang, Stability criteria for complex ecosystems. *Nature* **483**, 205–208 (2012).
13. A. Mougi, M. Kondoh, Diversity of interaction types and ecological community stability. *Science* **337**, 349–351 (2012).
14. S. Suweis, J. Grilli, A. Maritan, Disentangling the effect of hybrid interactions and of the constant effort hypothesis on ecological community stability. *Oikos* **123**, 525–532 (2014).
15. P. Chesson, N. Huntly, The roles of harsh and fluctuating conditions in the dynamics of ecological communities. *Am. Nat.* **150**, 519–553 (1997).
16. F. Carrara, F. Altermatt, I. Rodriguez-Iturbe, A. Rinaldo, Dendritic connectivity controls biodiversity patterns in experimental metacommunities. *Proc. Natl. Acad. Sci. U.S.A.* **109**, 5761–5766 (2012).
17. I. Hanski, Metapopulation dynamics. *Nature* **396**, 41–49 (1998).
18. J. E. Keymer, P. A. Marquet, J. X. Velasco-Hernández, S. A. Levin, Extinction thresholds and metapopulation persistence in dynamic landscapes. *Am. Nat.* **156**, 478–494 (2000).
19. O. Ovaskainen, K. Sato, J. Bascompte, I. Hanski, Metapopulation models for extinction threshold in spatially correlated landscapes. *J. Theor. Biol.* **215**, 95–108 (2002).
20. D. Alonso, A. McKane, Extinction dynamics in mainland-island metapopulations: An n-patch stochastic model. *Bull. Math. Biol.* **64**, 913–958 (2002).
21. R. V. Solé, D. Alonso, J. Saldaña, Habitat fragmentation and biodiversity collapse in neutral communities. *Ecol. Complex.* **1**, 65–75 (2004).

22. I. Hanski, O. Ovaskainen, The metapopulation capacity of a fragmented landscape. *Nature* **404**, 755–758 (2000).
23. I. Hanski, *Metapopulation Ecology* (Oxford Univ. Press, Oxford, 1999).
24. G. Nicoletti *et al*., Emergent encoding of dispersal network topologies in spatial metapopulation models. *Proc. Natl. Acad. Sci. U.S.A.* **120**, e2311548120 (2023).
25. T. R. Southwood, Habitat, the templet for ecological strategies? *J. Anim. Ecol.* **46**, 337–365 (1977).
26. R. Sole, J. Bascompte, *Self-Organization in Complex Ecosystems* (Princeton University Press, New York, 2006).
27. O. Ovaskainen, I. Hanski, "Metapopulation dynamics in highly fragmented landscapes" in *Ecology, Genetics and Evolution of Metapopulations*, I. Hanski, O. E. Gaggiotti, Eds. (Elsevier, 2004), pp. 73–103.
28. D. Urban, T. Keitt, Landscape connectivity: A graph-theoretic perspective. *Ecology* **82**, 1205–1218 (2001).
29. R. M. May, *Stability and Complexity in Model Ecosystems* (Princeton University Press, 2019), vol. 1.
30. P. A. Marquet *et al*., On theory in ecology. *BioScience* **64**, 701–710 (2014).
31. L. J. Gilarranz, J. Bascompte, Spatial network structure and metapopulation persistence. *J. Theor. Biol.* **297**, 11–16 (2012).
32. V. J. Ontiveros, J. A. Capitán, E. O. Casamayor, D. Alonso, Colonization-persistence trade-offs in natural bacterial communities. *Proc. R. Soc. B* **290**, 20230709 (2023).
33. B. Rayfield, C. B. Baines, L. J. Gilarranz, A. Gonzalez, Spread of networked populations is determined by the interplay between dispersal behavior and habitat configuration. *Proc. Natl. Acad. Sci. U.S.A.* **120**, e2201553120 (2023).
34. M. Holyoak, Habitat patch arrangement and metapopulation persistence of predators and prey. *Am. Nat.* **156**, 378–389 (2000).
35. M. Bevanda, E. A. Fronhofer, M. Heurich, J. Müller, B. Reineking, Landscape configuration is a major determinant of home range size variation. *Ecosphere* **6**, 1–12 (2015).
36. P. Staddon, Z. Lindo, P. D. Crittenden, F. Gilbert, A. Gonzalez, Connectivity, non-random extinction and ecosystem function in experimental metacommunities. *Ecol. Lett.* **13**, 543–552 (2010).
37. P. A. Arancibia, P. J. Morin, Network topology and patch connectivity affect dynamics in experimental and model metapopulations. *J. Anim. Ecol.* **91**, 496–505 (2022).
38. Y. Tao, A. Hastings, K. D. Lafferty, I. Hanski, O. Ovaskainen, Landscape fragmentation overturns classical metapopulation thinking. *Proc. Natl. Acad. Sci. U.S.A.* **121**, e2303846121 (2024).
39. P. L. Zarnetske *et al*., The interplay between landscape structure and biotic interactions. *Curr. Landsc. Ecol. Rep.* **2**, 12–29 (2017).
40. F. Roy, M. Barbier, G. Biroli, G. Bunin, Complex interactions can create persistent fluctuations in high-diversity ecosystems. *PLoS Comput. Biol.* **16**, e1007827 (2020).
41. M. T. Pearce, A. Agarwala, D. S. Fisher, Stabilization of extensive fine-scale diversity by ecologically driven spatiotemporal chaos. *Proc. Natl. Acad. Sci. U.S.A.* **117**, 14572–14583 (2020).
42. A. Altieri, G. Biroli, Effects of intraspecific cooperative interactions in large ecosystems. *SciPost Phys.* **12**, 013 (2022).
43. E. Mallmin, A. Traulsen, S. De Monte, Chaotic turnover of rare and abundant species in a strongly interacting model community. *Proc. Natl. Acad. Sci. U.S.A.* **121**, e2312822121 (2024).
44. M. Luo, S. Wang, S. Saavedra, D. Ebert, F. Altermatt, Multispecies coexistence in fragmented landscapes. *Proc. Natl. Acad. Sci. U.S.A.* **119**, e2201503119 (2022).
45. N. Anceschi *et al*., Neutral and niche forces as drivers of species selection. *J. Theor. Biol.* **483**, 109969 (2019).
46. D. Gravel, F. Massol, M. A. Leibold, Stability and complexity in model meta-ecosystems. *Nat. Commun.* **7**, 12457 (2016).
47. G. L. Giulia, A. Altieri, G. Biroli, Interactions and migration rescuing ecological diversity. *PRX Life* **2**, 013014 (2024).
48. J. W. Baron, T. Galla, Dispersal-induced instability in complex ecosystems. *Nat. Commun.* **11**, 6032 (2020).
49. R. Tamme, I. Hiiesalu, L. Laanisto, R. Szava-Kovats, M. Pärtel, Environmental heterogeneity, species diversity and co-existence at different spatial scales. *J. Veg. Sci.* **21**, 796–801 (2010).
50. J. Kehe *et al*., Positive interactions are common among culturable bacteria. *Sci. Adv.* **7**, eabi7159 (2021).
51. J. Grilli *et al*., Feasibility and coexistence of large ecological communities. *Nat. Commun.* **8**, 14389 (2017).
52. K. Gross, Positive interactions among competitors can produce species-rich communities. *Ecol. Lett.* **11**, 929–936 (2008).
53. P. Piccardi, B. Vessman, S. Mitri, Toxicity drives facilitation between 4 bacterial species. *Proc. Natl. Acad. Sci. U.S.A.* **116**, 15979–15984 (2019).
54. V. A. Jansen, J. Yoshimura, Populations can persist in an environment consisting of sink habitats only. *Proc. Natl. Acad. Sci. U.S.A.* **95**, 3696–3698 (1998).
55. G. Nicoletti, D. M. Busiello, Information propagation in multilayer systems with higher-order interactions across timescales. *Phys. Rev. X* **14**, 021007 (2024).
56. A. Posfai, T. Taillefumier, N. S. Wingreen, Metabolic trade-offs promote diversity in a model ecosystem. *Phys. Rev. Lett.* **118**, 028103 (2017).
57. M. Tikhonov, R. Monasson, Collective phase in resource competition in a highly diverse ecosystem. *Phys. Rev. Lett.* **118**, 048103 (2017).
58. N. Mouquet, M. Loreau, Coexistence in metacommunities: The regional similarity hypothesis. *Am. Nat.* **159**, 420–426 (2002).
59. M. Newman, *Networks* (Oxford University Press, 2018).
60. J. Dall, M. Christensen, Random geometric graphs. *Phys. Rev. E* **66**, 016121 (2002).
61. R. Rigon, A. Rinaldo, I. Rodriguez-Iturbe, R. L. Bras, E. Ijjasz-Vasquez, Optimal channel networks: A framework for the study of river basin morphology. *Water Resour. Res.* **29**, 1635–1646 (1993).
62. A. Rinaldo, R. Rigon, J. Banavar, A. Maritan, I. Rodriguez-Iturbe, Evolution and selection of river networks: Statics, dynamics, and complexity. *Proc. Natl. Acad. Sci. U.S.A.* **111**, 2417–2424 (2014).
63. L. Leopold, M. Wolman, J. Miller, *Fluvial Processes in Geomorphology* (Freeman, San Francisco, 1964).
64. I. Rodriguez-Iturbe, A. Rinaldo, *Fractal River Basins. Chance and Self-Organization* (Cambridge University Press, New York, 2001).
65. G. E. Hutchinson, The paradox of the plankton. *Am. Nat.* **95**, 137–145 (1961).
66. H. Zhang *et al*., Dispersal network heterogeneity promotes species coexistence in hierarchical competitive communities. *Ecol. Lett.* **24**, 50–59 (2021).
67. M. M. Herberich, S. Gayler, K. Tielbörger, Environmental heterogeneity promotes coexistence among plant life-history strategies through stabilizing mechanisms in space and time. *Basic Appl. Ecol.* **71**, 45–56 (2023).
68. T. Gibbs, S. A. Levin, J. M. Levine, Coexistence in diverse communities with higher-order interactions. *Proc. Natl. Acad. Sci. U.S.A.* **119**, e2205063119 (2022).
69. J. Nauta, M. De Domenico, Topological conditions drive stability in meta-ecosystems. arXiv [Preprint] (2024). http://arxiv.org/abs/2405.05390 (Accessed 4 October 2024).
70. M. Scheffer *et al*., Anticipating critical transitions. *Science* **338**, 344–348 (2012).
71. C. W. Gardiner *et al*., *Handbook of stochastic methods* (Springer, Berlin, 1985), vol. 3.
72. D. Montgomery, W. Dietrich, Where do channels begin? *Nature* **336**, 232–234 (1988).
73. J. Banavar, F. Colaiori, A. Flammini, A. Maritan, A. Rinaldo, Scaling, optimality, and landscape evolution. *J. Stat. Phys.* **104**, 1–48 (2001).
74. L. Carraro *et al*., Generation and application of river network analogues for use in ecology and evolution. *Ecol. Evol.* **10**, 7537–7550 (2020).